Available online at www.sciencedirect.com
ScienceDirect
Catalysis Today 121 (2007) 226–236
CATALYSIS TODAY
www.elsevier.com/locate/cattod

# TAP study of NOx storage and reduction on $Pt/Al_2O_3$ and $Pt/Ba/Al_2O_3$ ☆

Vinay Medhekar, Vemuri Balakotaiah **, Michael P. Harold *

*Department of Chemical Engineering, University of Houston, Houston, TX 77204-4004, USA*

Available online 27 September 2006

**Abstract**

A systematic mechanistic study of NO storage and reduction over $Pt/Al_2O_3$ and $Pt/BaO/Al_2O_3$ is carried out using Temporal Analysis of Products (TAP). NO pulse and $NO/H_2$ pump-probe experiments at 350 °C on pre-reduced, pre-oxidized, and pre-nitrated catalysts reveal the complex interplay between storage and reduction chemistries and the importance of the Pt/Ba coupling. NO pulsing experiments on both catalysts show that NO decomposes to major product $N_2$ on clean Pt but the rate declines as oxygen accumulates on the Pt. The storage of NO over $Pt/BaO/Al_2O_3$ is an order of magnitude higher than on $Pt/Al_2O_3$ showing participation of Ba in the storage even in the absence of gas phase $O_2$. Either oxygen spillover or transient NO oxidation to $NO_2$ is postulated as the first steps for NO storage on $Pt/BaO/Al_2O_3$. The storage on $Pt/Ba/Al_2O_3$ commences as soon as Pt–O species are formed. Post-storage $H_2$ reduction provides evidence that a fraction of NO is not stored in close proximity to Pt and is more difficult to reduce. A closely coupled Pt/Ba interfacial process is corroborated by $NO/H_2$ pump-probe experiments. NO conversion to $N_2$ by decomposition is sustained on clean Pt using excess $H_2$ pump-probe feeds. With excess NO pump-probe feeds NO is converted to $N_2$ and $N_2O$ via the sequence of barium nitrate and NO decomposition. Pump-probe experiments with pre-oxidized or pre-nitrated catalyst show that $N_2$ production occurs by the decomposition of NO supplied in a NO pulse or from the decomposition of NOx stored on the Ba. The transient evolution of the two pathways depends on the extent of pre-nitration and the $NO/H_2$ feed ratio.


*Keywords:* NOx; Lean NOx trap; Selective catalytic reduction; Platinum; Barium

## 1. Introduction

Lean-burn vehicles afford reduced fuel consumption compared to stoichiometric gasoline vehicles. But their exhaust has more $O_2$, making it difficult to reduce NOx by conventional three way catalysis. NOx storage and reduction (NSR), first conceived by Toyota [1–3], is a promising technology for reducing the NOx emissions in such vehicles. NSR itself is operated by an alternating protocol, involving a lean period of 30–90 s duration in which exhaust NOx is stored on the catalyst, followed by an abbreviated, 3–5 s rich pulse which reduces the stored NOx. The desired products are $N_2$, $CO_2$ and $H_2O$, although undesired formation of byproducts like $N_2O$ and $NH_3$ are encountered. Typical NSR catalysts consist of a precious metal component (Pt, Pd, Rh) and a storage component from the family of alkali earth metals (Ba, K, Sr, Ca).

The NSR storage and reduction chemistry is highly complex due in part to its inherently transient operation, multi-functional catalysts, and coupled reaction and transport processes [4–9]. Recent studies suggest that both storage and reduction occur in close proximity to the Pt/Ba interface [10,11]. A spillover mechanism involving oxygen from Pt to Ba and reverse spillover of NOx from the stored nitrite/nitrate to Pt have been postulated to occur for the storage and reduction steps, respectively [11–13]. Nova et al. [14] have shown that the NOx storage and reduction is improved when the Pt is in closer proximity to the Ba [14]. Sakamoto et al. [13] have demonstrated using a spatially resolved spectroscopic technique that NOx storage and reduction occurs at the Pt–Ba interface.

☆ This report was prepared as an account of work sponsored by an agency of the United State Government. Neither the United States Government nor any agency thereof, nor any of their employees, makes any warranty, express or implied or assumes any legal liability or responsibility for the accuracy, completeness, or usefulness of any information, apparatus, product, or process disclosed, or represents that its use would not infringe privately owned rights. References herein to any specific commercial product, process, or service by trade name, trademark, manufacturer, or favoring by the United States Government or any agency thereof. The views and opinions of authors expressed herein do not necessarily state or reflect those of the United States Government or any agency thereof.

* Corresponding author. Tel.: +1 713 743 4307.
** Corresponding author. Tel.: +1 713 743 4318.
*E-mail addresses:* bala@uh.edu (V. Balakotaiah), mharold@uh.edu (M.P. Harold).

0920-5861/$ – see front matter © 2006 Elsevier B.V. All rights reserved.
doi:10.1016/j.cattod.2006.08.063

Most previous studies of NSR have been carried out using conventional atmospheric pressure flow reactors containing model powder or monolith catalysts. The complicating effects of transport limitations and nonisothermal effects together with the multiple overall reactions makes the interpretation of NSR data a challenge. Considerable progress has been made in complementary kinetic and reactor modeling [15–18]. Studies are needed to decouple the primary reactions and to minimize transport effects in order to extract intrinsic kinetic and mechanistic information. Temporal Analysis of Products (TAP) is one such approach that avoids the disadvantages of traditional flow and integral reactors [19,20]. TAP affords the ability to conduct transient experiments under constant catalyst state conditions. This provides crucial kinetic data on the highly complex NSR process. To this end, the inherent transient operation of TAP makes it a suitable tool to study the NSR catalytic process. In the current study, we perform systematic TAP experiments of NOx storage and reduction using a combination of pulse and pump-probe experiments on model $Pt/Al_2O_3$ and $Pt/BaO/Al_2O_3$ catalysts. The experiments help to elucidate the important effects of oxygen inhibition, the formation of byproducts $N_2$, $N_2O$ and $NH_3$, and the coupling between Pt and Ba functions. It also provide a basis for mechanism development and kinetic parameter estimation, for which the current experimental study is a first step.

## 2. Experimental

Two catalyst powders provided by Engelhard Inc. were used for this study: 1.52 wt.% $Pt/Al_2O_3$ (A) and 1.27 wt.% Pt/16.5 wt.% $BaO/Al_2O_3$ (B). Detailed characteristics of the catalysts are provided in Table 1. About 90 mg of undiluted catalyst was positioned between two zones containing quartz beads. For the given Pt loading and dispersion, this corresponded to about $1.3 \times 10^{18}$ exposed Pt atoms for catalyst A and $1.2 \times 10^{18}$ atoms for catalyst B.

The TAP® Generation-1 reactor system used in this study is described in more detail elsewhere [5]. Both pulse and pump-probe experiments were conducted. The amount of pulsed gas was determined by monitoring the pressure loss in the feed bulb. A quadrupole mass spectrometer was used to quantify the molecular flow rates of the product gases. Species measured included NO ($m/e = 30$), $N_2$ ($m/e = 28$), $N_2O$ ($m/e = 44.4$), $NH_3$ ($m/e = 16.9$), and $H_2O$ ($m/e = 17.9$). Both storage and storage/reduction experiments were conducted as follows.

Table 1
Properties of the two catalyst samples used in the TAP reactor

| Sample | $Pt/Al_2O_3$ | $Pt/BaO/Al_2O_3$ |
|---|---|---|
| Pt (wt%) | 1.52 | 1.27 |
| BaO (wt%) | 0 | 16.5 |
| Pt dispersion (%) | 30.4 | 33.0 |
| Pt area ($m^2/g$) | 1.14 | 1.04 |
| Pt particle size (nm) | 3.72 | 3.43 |
| Estimated no. of Pt sites exposed in 90 mg of catalyst | $1.27 \times 10^{18}$ | $1.16 \times 10^{18}$ |

### 2.1. NO storage and reduction

Prior to NO storage, the catalysts were pre-reduced in $H_2$ at 400–450 °C for 2–4 h. NO was then pulsed over catalysts A and B at 350 °C for a prescribed period. The series of NO pulses were separated by 4 s intervals, which exceeds the estimated characteristic diffusion time of 2 s over an inert bed. The amount of NO introduced varied from $1 \times 10^{16}$ to $4 \times 10^{16}$ molecules/pulse, which is considerably less than the number of exposed Pt atoms. The amount of N stored was determined by the difference in the amount of NO pulsed and the amount of N in the product species. After storage, the catalyst was exposed to a series of $H_2$ pulses at the same temperature to study the reduction of stored NO, maintaining the isothermal conditions.

### 2.2. NO pump-probe

A similar catalyst pretreatment was conducted prior to $NO/H_2$ pump-probe experiments. The pump-probe involved feeding alternating pulses of NO and $H_2$. Each pulse of NO and $H_2$ were separated by 4–6 s. The opening time for each pulse ranged from 200 to 600 μs depending on the desired $NO:H_2$ feed ratio. Three types of pump-probe experiments were carried out. In the *pre-reduced* pump-probe experiments the catalyst surface was cleaned of adsorbed species by a reduction at 400 °C with $H_2$ for 2 h. In the *pre-oxidized* pump-probe experiments, the pre-reduced catalyst was exposed to sequential pulses of $O_2$ at 450 °C for 2 h, with each pulse separated by 4 s. In the *pre-nitrated* pump-probe experiments, the pre-reduced catalyst was exposed to 2000 pulses of NO. All pump-probe experiments were conducted at 350 °C; previous studies have shown that NOx storage on Pt/Ba catalysts is highest in the 300–350 °C temperature range [5,7]. Moreover, diesel engine exhaust temperatures are typically in the 200–400 °C range after startup.

## 3. Results

NO storage results over $Pt/Al_2O_3$ (catalyst A) and $Pt/BaO/Al_2O_3$ (catalyst B) are shown in Fig. 1a and b, respectively. The average pulse size over catalyst A was $1.40 \times 10^{16}$ molecules/pulse and $1.83 \times 10^{16}$ molecules/pulse for catalyst B. The pulse intensity decreased with pulse number because of the reduced NO feed pressure in the inlet system (fixed valve opening time). Species measured included $N_2$, $N_2O$ as well as untrapped/unconverted NO. The data enable an estimate of the fraction of NO fed that is converted to $N_2$ and $N_2O$ and the fraction that is stored or consumed. The stored amount is obtained by subtracting the total measured N out $[(NO)_{out} + 2(N_2)_{out} + 2(N_2O)_{out}]$ from the total NO fed. For both catalysts, the first few NO pulses resulted in the formation of $N_2$, a comparatively much smaller amount of $N_2O$, but no NO. NO breakthrough was observed at about the 55th pulse for catalyst A and about the 30th pulse for catalyst B. The increase of NO just after breakthrough was sharper for $Pt/Al_2O_3$ than for $Pt/BaO/Al_2O_3$. While the output NO for both catalysts increased towards the feed value, the rate of increase for B was much more gradual than for A. Moreover, the total N approached more closely to the feed value

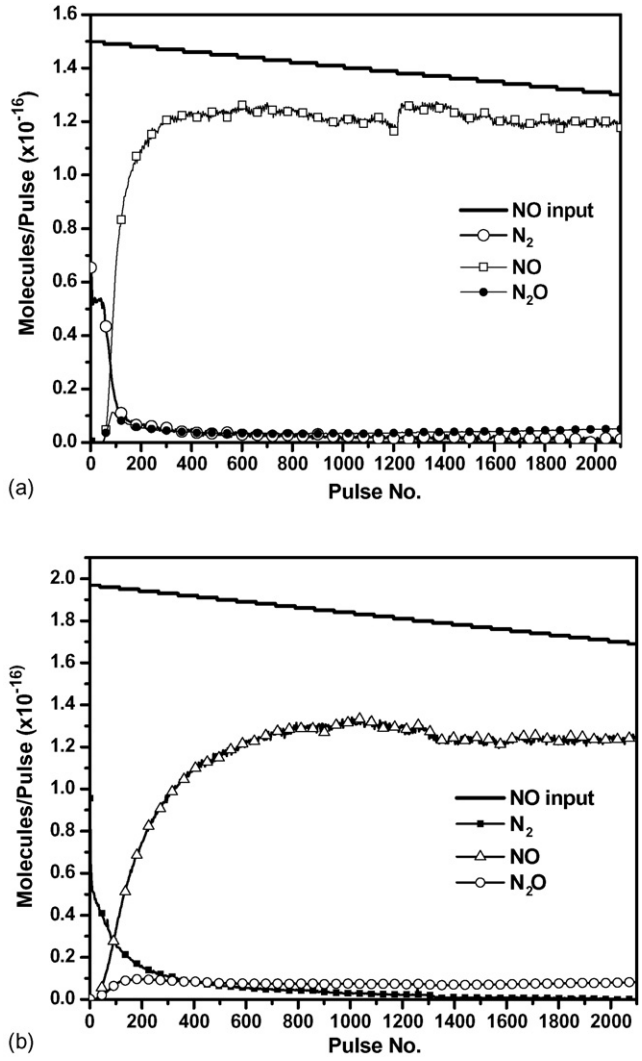


Fig. 1. (a) NO storage over $Pt/Al_2O_3$ at 350 °C, (b) NO storage over $Pt/BaO/Al_2O_3$ at 350 °C.

for catalyst A than for catalyst B, indicating more storage for B than A. The $N_2$ formation decreased monotonically with pulse number after the maximum, which occured at the first pulse for catalysts A and B. In our previous work [5], we have shown for a much smaller pulse size ($\sim 1 \times 10^{15}$ molecules/pulse) that $N_2$ formation exhibits a maximum at an intermediate pulse number. A sharp increase in the $N_2O$ formation was observed at the point of breakthrough of NO. The $N_2O$ achieved a maximum and then decreased. The decrease in $N_2O$ was rather sharp for catalyst A, whereas for catalyst B the $N_2O$ exhibited only a slight drop and was sustained at a nonzero value throughout the remainder of the experiment.

Table 2
NO storage over $Pt/Al_2O_3$ and $Pt/BaO/Al_2O_3$ as calculated from the data in Fig. 1a and b (storage) and Fig. 2 (reduction)

| Catalyst | $Pt/Al_2O_3$ | $Pt/BaO/Al_2O_3$ |
|---|---|---|
| N storage during NO pulse (mol N/g cat) | $3.0 \times 10^{-5}$ | $1.5 \times 10^{-4}$ |
| Storage estimated from $N_2$ out (mol N/g cat) | $3.6 \times 10^{-6}$ | $4.2 \times 10^{-5}$ |

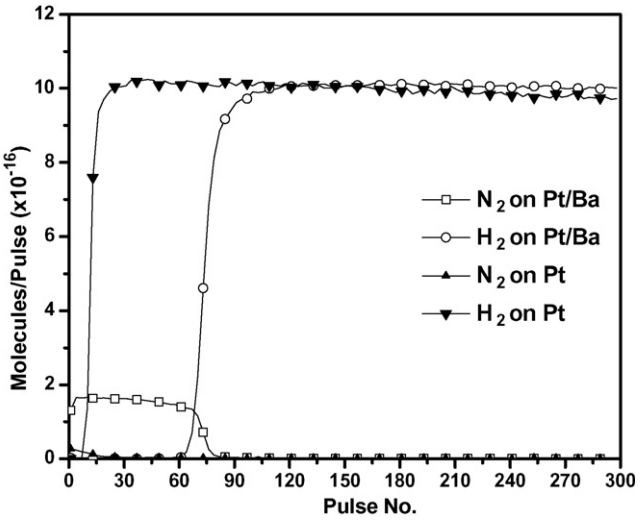


Fig. 2. Nitrogen and hydrogen effluent flow profiles during reduction of pre-nitrated $Pt/Al_2O_3$ and $Pt/BaO/Al_2O_3$.

The post-storage reduction provides additional information about the extent of storage and of the reduction chemistry. Fig. 2 shows the results of the post-storage reduction of each catalyst after 2100 pulses of NO. The reduction temperature was 350 °C and each $H_2$ pulse comprised about $8.1 \times 10^{16}$ molecules. For catalyst A, negligible production of $N_2$ was observed compared to the more pronounced $N_2$ production for catalyst B, indicating again the higher storage on $Pt/BaO/Al_2O_3$ compared to $Pt/Al_2O_3$ (Table 2). A complete scan of the effluent revealed the production of ammonia and water (Fig. 3). Nitrogen was the dominant product during the first few pulses but dropped to the detection limit by the 100th pulse. The amount of $N_2$ released during reduction corresponded to a storage of $2.1 \times 10^{-5}$ mol/g cat. The breakthrough of $H_2$ occured during the drop in $N_2$. Within the cross-over region of the $N_2/H_2$ a maximum in $NH_3$ formation was observed. The late appearance of ammonia and water may be a result of slow desorption from the porous catalyst or adsorption to the walls of the apparatus.

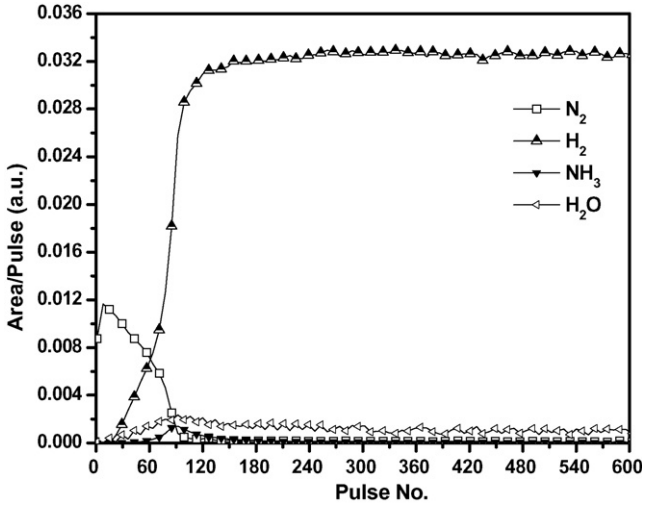


Fig. 3. Nitrogen, hydrogen, ammonia, and water effluent profiles during reduction of pre-nitrated $Pt/BaO/Al_2O_3$.

The results of the pump-probe experiments on the pre-reduced $Pt/BaO/Al_2O_3$ catalyst are shown in Fig. 4a–c corresponding to three different $NO:H_2$ feed ratios; specifically, $NO:H_2$ = 1:3.8 (Fig. 4a), 1:0.50 (Fig. 4b), 1:0.34 (Fig. 4c).

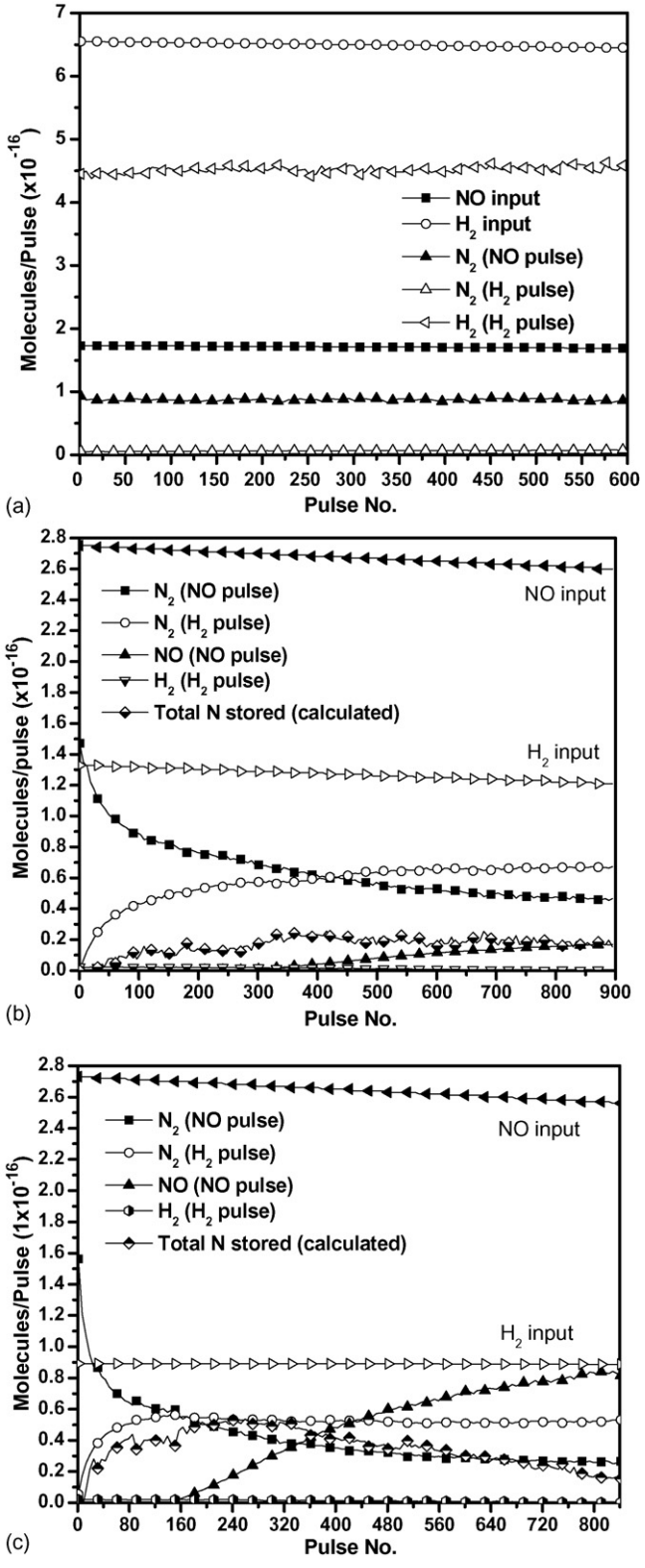


Fig. 4. (a) NO–$H_2$ pump-probe on pre-reduced $Pt/BaO/Al_2O_3$ for $NO:H_2$ = 1:3.8. (b) NO–$H_2$ pump-probe over pre-reduced $Pt/BaO/Al_2O_3$ for $NO:H_2$ = 1:0.5. (c) Effluent molecular flow profiles for $NO:H_2$ = 1:0.34.

When $H_2$ was in excess of NO (Fig. 4a; average feed values: NO = $1.71 \times 10^{16}$ molecules/pulse, $H_2$ = $6.50 \times 10^{16}$ molecules/pulse), there was little change in the results over the course of the 300 pump-probe pair experiment. The first NO pulse produced was about half the amount of $N_2$, and was maintained at a nearly constant level with subsequent NO pulses. This shows that the $H_2$ pulse is effective in returning the Pt to its initial reduced state. The excess $H_2$ that remained from the reaction is seen during the $H_2$ pulse. The production of negligible $N_2$ (below detection level) during the $H_2$ pulse indicates that little N was adsorbed on Pt or stored on the barium phase for additional $N_2$ production. Subsequent pump-probe pairs led to the same result; i.e., the NO pulse produced $N_2$ equivalent to the previous pump-probe cycle.

If less $H_2$ was pulsed than NO ($NO:H_2$ = 1:0.50 in Fig. 4b; average feed values: NO = $2.50 \times 10^{16}$, $H_2$ = $1.27 \times 10^{16}$), the results were much different over the course of the experiment. The first NO pulse produced $N_2$ on the pre-reduced Pt surface. This feature is similar to the excess $H_2$ pump-probe experiment. However, the first $H_2$ pulse also produced $N_2$, albeit a much smaller amount. Subsequent pump-probe pairs resulted in an apparent $H_2$ reduction of NO stored on the barium phase (i.e., during NO pulse). While $N_2$ continued to be generated during the NO pulse, the amount decreased with pulse number while the amount of $N_2$ generated during the $H_2$ pulse increased with pulse number. The results also reveal the breakthrough of NO concurrent with the decrease in $N_2$ production during the NO pulse. An indication that there is insufficient $H_2$ is its absence in the product during the $H_2$ pulse. Apparently $H_2$ was completely consumed during the reduction process and it is this imbalance that led to the continued decrease (increase) in $N_2$ production during the NO ($H_2$) pulse. An experiment with even less $H_2$ was conducted, the results of which are shown in Fig. 4c ($NO:H_2$ = 1:0.34; average feed values: NO = $2.64 \times 10^{16}$ molecules/pulse, $H_2$ = $8.90 \times 10^{15}$ molecules/pulse). A more pronounced decrease in the $N_2$ production with pulse number was observed during the NO pulse. The production of $N_2$ during the $H_2$ pulse increased more sharply to a constant

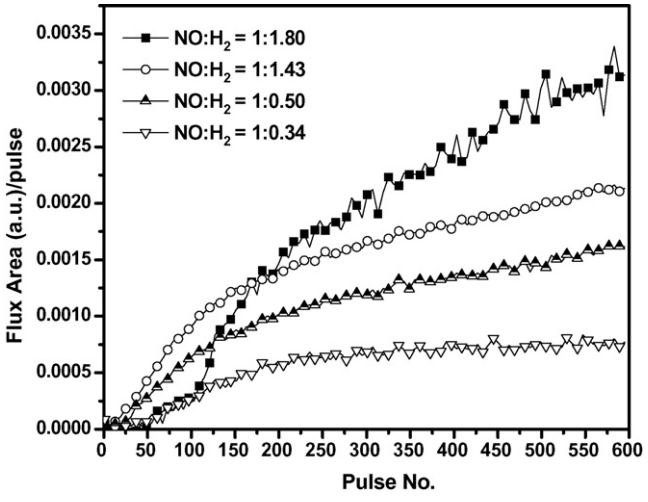


Fig. 5. Ammonia production for four $NO:H_2$ feed ratios.

level by the 200th pulse. In addition, the breakthrough of unreacted/untrapped NO occured much earlier and was more significant. The amount of $N_2$ generated during the $H_2$ pulse is clearly a function of the amount of $H_2$ introduced relative to NO and is close to 0.5 at pseudo-steady state.

The production of byproduct ammonia was observed during the pump-probe experiments. Fig. 5 shows the production of $NH_3$ as a function of pulse number for several different NO:$H_2$ ratios. As the $H_2$ feed with respect to NO was increased, the $NH_3$ production increased. While the data showed the production of ammonia during both the NO and $H_2$ pulses, we cannot rule out a slow ammonia release.

In order to understand the effect of an oxidized surface on the storage and reduction process, we carried out a set of pump-probe experiments on pre-oxidized Pt/BaO/$Al_2O_3$ catalyst with excess $H_2$ (NO:$H_2$ = 1:2.4; average feed values: NO = $2.40 \times 10^{16}$ molecules/pulse, $H_2 = 5.84 \times 10^{16}$ molecules/pulse). Fig. 6a shows the overall trend of products formed during both the NO and $H_2$ pulses. As seen clearly in Fig. 6b, negligible formation of $N_2$ was observed during the first ca. 15 NO pulses. With the excess $H_2$ the Pt surface was cleaned during the subsequent $H_2$ pulse, freeing Pt sites for NO decomposition. During the first few pulses of $H_2$ (Fig. 6b), production of $N_2$ was observed but declined in intensity. The $N_2$ produced decreased to zero on further reduction with simultaneous breakthrough of $H_2$. After the first ca. 30 pulses, the results resembled those for excess $H_2$ on the pre-reduced catalyst (Fig. 4a).

In order to further our understanding of the reduction process, pump-probe experiments were carried out on a pre-nitrated Pt/BaO/$Al_2O_3$ catalyst. In this experiment the catalyst was exposed to about 2100 pulses of NO before switching to a NO/$H_2$ pump-probe protocol. The pretreatment created a Pt/BaO/$Al_2O_3$ catalyst with a prescribed amount of stored nitrogen (approximately $1.6 \times 10^{-4}$ mol N/g cat).

The excess $H_2$ pump-probe exposed the pre-nitrated Pt/BaO/$Al_2O_3$ catalyst to a net reducing cycle (Fig. 7a and b). The first NO pulse led to NO breakthrough with negligible $N_2$ production. The following $H_2$ pulse led to significant production of $N_2$,

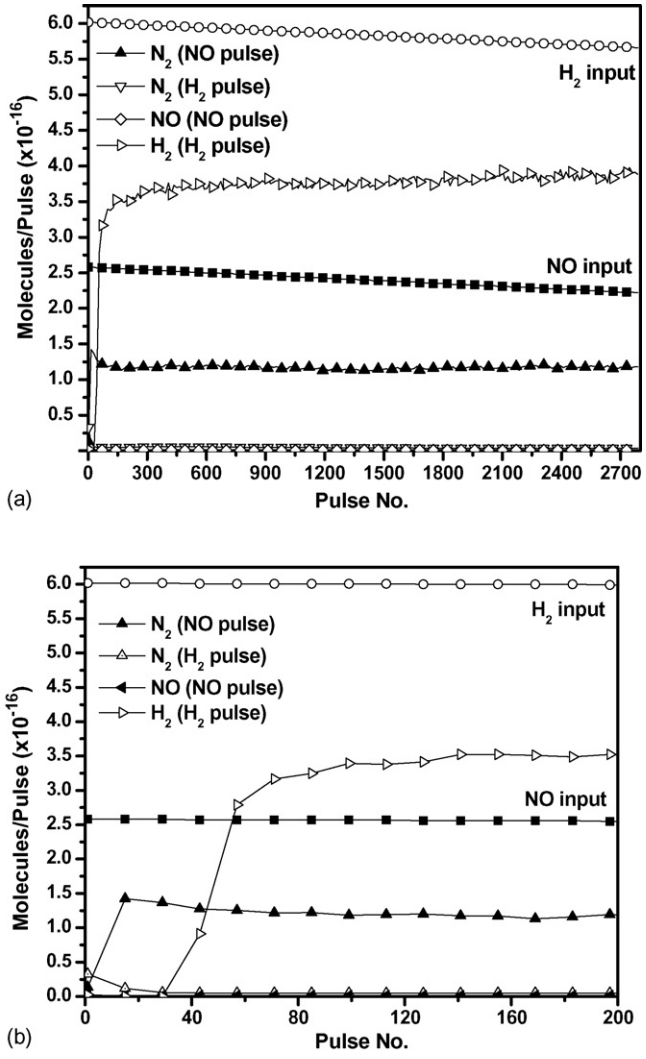


Fig. 6. (a) NO–$H_2$ pump-probe for NO:$H_2$ = 1:2.5 over pre-oxidized catalyst. (b) Expanded view of data from (a).

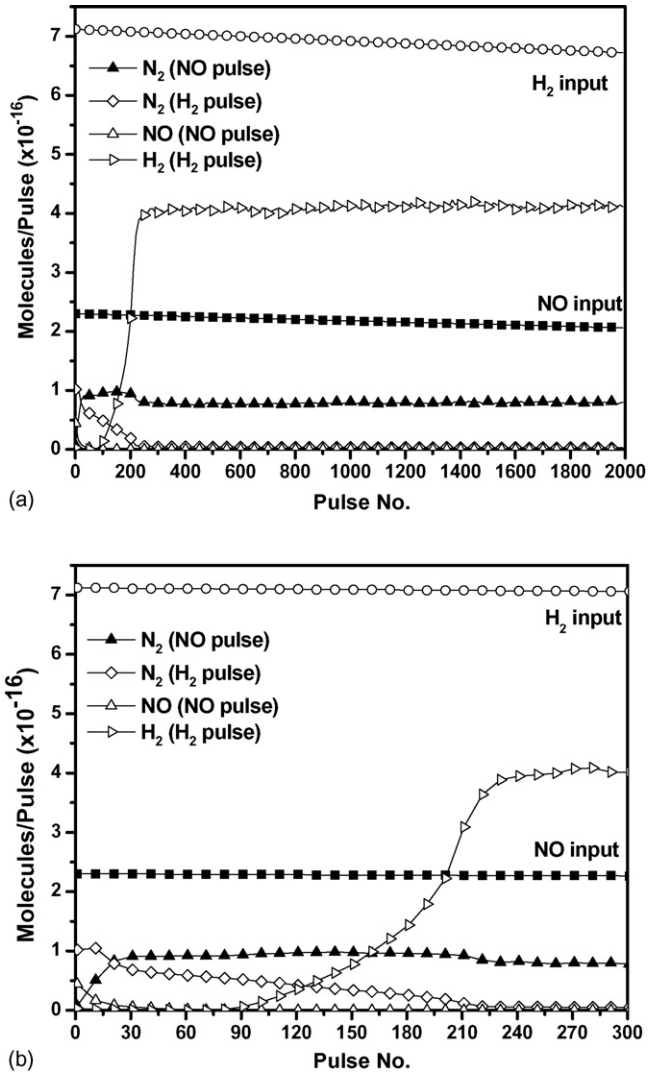


Fig. 7. (a) Effluent species profiles for NO:$H_2$ = 1:3.14 pump-probe experiment for a pre-nitrated catalyst. (b) Expanded view of data from (a).

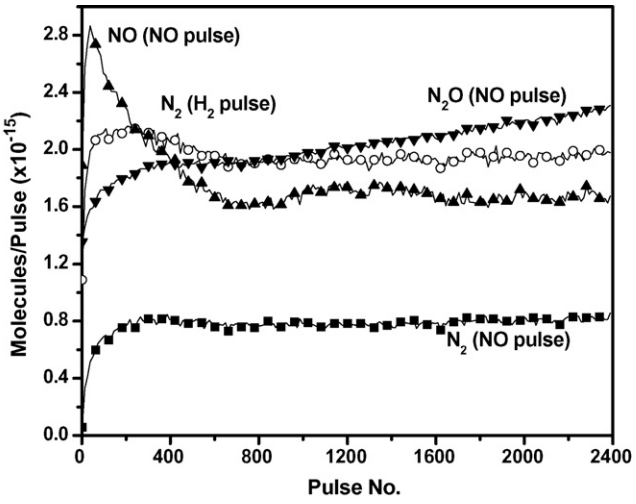


Fig. 8. NO–$H_2$ pump-probe over Pt/BaO/$Al_2O_3$ in excess of NO.

presumably of N pre-stored on the catalyst. Subsequent pump-probe pairs led to an increased production of $N_2$ during the NO pulse and reduced $N_2$ production during the $H_2$ pulse, as the overall cycle was net-reducing. Eventually the results resembled those of the pre-reduced catalyst exposed to the excess $H_2$ pump-probe (Fig. 4a). By the 200th pulse a pseudo-steady state was reached in which $N_2$ was produced primarily during the NO pulse, with a negligible amount formed during the $H_2$ pulse. $H_2$ breakthrough occured at the time when overall N stored over catalyst was reduced, similar to the results obtained during the reduction process shown in Fig. 2.

The excess NO pump-probe experiments on the pre-nitrated Pt/BaO/$Al_2O_3$ catalyst lead to a different set of results (Fig. 8). There was a similar initial breakthrough of NO during the NO pulse as in the previous excess $H_2$ case, indicating the inability of the pre-nitrated catalyst to effectively store NO. In subsequent pump-probe pairs, the NO breakthrough decreased, but not to zero in this case. Rather, the $N_2$ produced during the $H_2$ pulse increased to a sustained level while negligible $N_2$ was produced during the NO pulsing. The $N_2O$ production was more pronounced in this case. By the 500th pulse a pseudo-steady state was reached in which $N_2$ was produced during the $H_2$ pulse.

## 4. Discussion

The TAP storage and reduction data provide the basis for building an understanding of the mechanism and for constructing predictive microkinetic models. While our ultimate goal is to estimate kinetic parameters, here we outline such a model that is consistent with the data that builds on recent results from the literature.

### 4.1. Storage

The exposure of NO to the Pt/$Al_2O_3$ and Pt/BaO/$Al_2O_3$ reveals a combination of both NO decomposition and adsorption/storage. The following mechanism for NO decomposition on Pt is proposed:

$$NO + Pt \leftrightarrow NO{-}Pt \quad (S1)$$

$$NO{-}Pt + Pt \leftrightarrow N{-}Pt + O{-}Pt \quad (S2)$$

$$2N{-}Pt \leftrightarrow N_2 + 2Pt \quad (S3)$$

$$2NO{-}Pt \leftrightarrow N_2O + Pt + O{-}Pt \quad (S4)$$

$$NO{-}Pt + N{-}Pt \leftrightarrow N_2O + 2Pt \quad (S5)$$

$$NO{-}Pt + O{-}Pt \leftrightarrow NO_2 + 2Pt \quad (S6)$$

$$O{-}Pt + O{-}Pt \leftrightarrow O_2 + 2Pt \quad (S7)$$

This mechanism is consistent with NO pulse data for both Pt/$Al_2O_3$ and Pt/BaO/$Al_2O_3$ (Fig. 1a and b) and follows from developments in our previous study [5]. A key feature of this mechanism is the inhibition by accumulating oxygen adatoms which do not readily desorb because of the high binding energy of oxygen on Pt (200–240 kJ/mol); i.e., the rate of forward reaction (S7) is negligible at temperatures below 400 °C. As NO is pulsed over the catalyst, the oxygen accumulation reduces the availability of vacant sites on Pt for NO adsorption (S1), NO bond scission (S2), and N adatom recombination (S3). On the initially clean Pt surface the first few pulses of NO produce a near-stoichiometric amount of $N_2$ (2NO produce $1N_2$). On Pt/$Al_2O_3$ the $N_2$ production and NO breakthrough occur more sharply than on Pt/BaO/$Al_2O_3$. As we discuss later, oxygen adatoms on Pt in the vicinity of the Pt–BaO interface may participate in the storage of NO. This frees up additional Pt sites, enabling the storage process to continue. As oxygen builds up on Pt, this leads to fewer vacant sites. As a result, the rate of NO bond scission decreases and fewer N adspecies are produced. On this more crowded surface $N_2O$ formation occurs via steps (S4) or (S5), both of which generate vacant sites, enabling additional NO to adsorb and react. At the point in which few vacant Pt sites are available for NO adsorption, NO breakthrough occurs. This occurs about the same point in which the $N_2O$ production reaches a maximum.

A comparison of the Pt/$Al_2O_3$ and Pt/BaO/$Al_2O_3$ catalysts reveal some differences. The uptake of NO, being less on Pt/$Al_2O_3$ than on Pt/BaO/$Al_2O_3$, is an expected result because of the known capability of BaO to store NO even without gas phase $O_2$ [21]. Simultaneous decomposition and storage of NO occur on the Pt/BaO/$Al_2O_3$, leading to a more gradual breakthrough of NO. The $N_2$ production is sustained for a longer sequence of NO pulses for Pt/BaO/$Al_2O_3$, as is the $N_2O$ production.

Following our recent work and that of others, two storage pathways are consistent with the data. The first involves close coupling between the Pt and BaO [5,10,22]:

$$O{-}Pt + BaO \leftrightarrow BaO_2 + Pt \quad (S8)$$

$$BaO_2 + NO(-Pt) \leftrightarrow BaO{-}NO_2 + (Pt) \quad (S9)$$

$$BaO{-}NO_2 + NO(-Pt) \leftrightarrow Ba(NO_2)_2 + (Pt) \quad (S10)$$

$$Ba(NO_2)_2 + 2O{-}Pt \leftrightarrow Ba(NO_3)_2 + 2Pt \quad (S11)$$

In the absence of gas phase $O_2$, this pathway infers the spillover of oxygen adatoms from the Pt to Ba phase, producing $BaO_2$. This $O_2$ spillover pathway is speculative since the energy barrier for the oxygen spillover and oxidation of BaO has not been determined. The $BaO_2$ then undergoes deeper nitration by reaction with either gas phase NO or adsorbed NO which diffuses from the Pt crystallites. The barium nitrite can be further oxidized by additional surface oxygen, forming barium nitrate. The oxygen spillover processes ((S8) and (S11)) free up Pt sites for further NO adsorption and decomposition. Since oxygen is supplied by the dissociating NO, this helps to explain the slow breakthrough of NO with sustained production of $N_2$ as well as the sustained production of $N_2O$; i.e., Pt sites are made available for a longer period in the case of $Pt/BaO/Al_2O_3$ compared to $Pt/Al_2O_3$. $N_2O$ formation results in the generation of new vacant Pt sites which can result in further NO adsorption and decomposition. The constant, nonzero level of $N_2O$ production beyond the maximum indicates that sufficient NO is stored that a pseudo steady state can be established. It may also suggest that some storage of NO on the support occurs.

A second potential pathway involves $NO_2$ as the stored species, transported along the surface or through the gas phase:

$$NO_2(-Pt) + BaO \leftrightarrow BaO{-}NO_2 + (Pt) \quad \text{(S12)}$$

$$BaO{-}NO_2 + (Pt) \leftrightarrow BaO_2 + NO(-Pt) \quad \text{(S13)}$$

$$BaO_2 + NO_2(-Pt) \leftrightarrow BaO{-}NO_3 + (Pt) \quad \text{(S14)}$$

$$BaO{-}NO_3 + NO_2(-Pt) \leftrightarrow Ba(NO_3)_2 + (Pt) \quad \text{(S15)}$$

Note that the Pt shown in parenthesis indicates its possible, but not essential, role. This pathway requires the formation of $NO_2$ from NO in the absence of gas phase $O_2$ (reaction step (S6)). Consider the two overall reactions of NO decomposition and NO oxidation:

$$NO \leftrightarrow 0.5N_2 + 0.5O_2 \quad (1)$$

$$NO + 0.5O_2 \leftrightarrow NO_2 \quad (2)$$

The sum of these two reactions is NO disproportionation:

$$2NO \leftrightarrow NO_2 + 0.5N_2 \quad (3)$$

As we know, the catalytic decomposition of NO (1), while thermodynamically feasible, is kinetically hindered by oxygen inhibition. Moreover, NO oxidation is kinetically unfavorable below ca. 250 °C and encounters thermodynamic limitations for temperatures exceeding 400 °C. Thus, one would not expect significant production of $NO_2$ from NO in the absence of $O_2$ in the feed. However, under transient conditions in which accumulation of O occurs on the Pt surface, the pathway may become more significant. Similar to the oxygen spillover mechanism, storage of NO on BaO will result in the freeing up of Pt sites which in turn allow further adsorption and decomposition of NO, consistent with the data. Also, $NO_2$ formed on Pt may desorb from the Pt to react with BaO sites removed from the Pt sites.

In summary, NO storage may occur on Ba sites near Pt by the spillover mechanism and away from Pt sites by the $NO_2$ formation mechanism. Kinetic modeling currently underway in our group will help to resolve some of these questions.

After the 2000th pulse in case of $Pt/Al_2O_3$ the consumption of NO indicates about 15% is not accounted for in terms of output NO (Fig. 1a). For $Pt/Ba/Al_2O_3$ this amount is about 25%. This indicates that storage is still occurring even after 2000 NO pulses in the case of $Pt/Ba/Al_2O_3$. In the absence of BaO, we suspect that NO oxidation over Pt with adsorbed O to form $NO_2$ or adsorption on the alumina support may play a minor role in the unaccounted NO [23].

### 4.2. Reduction

The post-storage reduction data reveal the production of $N_2$ and $NH_3$ as well as the breakthrough of $H_2$ (Figs. 2 and 3). The reduction of $Pt/BaO/Al_2O_3$ produces more $N_2$ ($4.2 \times 10^{-5}$ mol N/g cat) as compared to $Pt/Al_2O_3$ ($3.6 \times 10^{-6}$ mol N/g cat) confirming that the BaO provides a storage function in the absence of oxygen. Two observations warrant discussion. First, the amount of generated $N_2$ is less than the amount of N that has stored over $Pt/Ba/Al_2O_3$ ($1.5 \times 10^{-4}$ mol N/g cat); i.e., about 28% of the amount stored. Some of the discrepancy is attributed to the co-generation of ammonia, which is not quantified in the N balance. Another factor, which we elaborate on below, has to do with the accessibility of stored NOx to the Pt. Second, for $Pt/BaO/Al_2O_3$ the ratio of the moles of $H_2$ consumed to the moles $N_2$ produced is about 5 over the course of the reduction (Fig. 2). This ratio is consistent with the stoichiometry of barium nitrate reduction:

$$Ba(NO_3)_2 + 5H_2 \leftrightarrow BaO + N_2 + 5H_2O \quad (4)$$

This lends credence to the aforementioned storage pathways that involve the formation of barium nitrate during exposure of NO. We speculate that the oxygen spillover and NO oxidation to $NO_2$ occur simultaneously during NO storage over Pt/Ba, although sufficient adsorbed O must be available for the latter to occur. On $Pt/Al_2O_3$, the storage as estimated by $N_2$ production during reduction is an order of magnitude lower, about $3.6 \times 10^{-6}$ mol N/g cat compared to $3.0 \times 10^{-5}$ mol N/g cat stored during NO pulsing.

### 4.3. Storage and reduction

The pump-probe data provide detailed insight into the surface chemistry. The products include $N_2$, $H_2O$, $NH_3$ and $N_2O$. In most of the experiments $N_2$ is the major N–containing product while byproduct $N_2O$ appears only after sufficient oxygen has accumulated. $NH_3$ appears only under reducing conditions. The pump-probe data shows that the main role of $H_2$ is to react with oxygen adatoms by the overall reaction:

$$H_2 + 0.5O_2 \leftrightarrow H_2O \quad (5)$$

Hydrogen oxidation cleans the surface for subsequent NO decomposition (1). The oxygen required for water formation is supplied during the NO decomposition ((S1)–(S3)), which

when combined with (5) yields the following overall reaction:

$$NO + H_2 \leftrightarrow 0.5N_2 + H_2O. \quad (6)$$

Adsorbed N species or NO may directly react with adsorbed H to form $NH_3$. The evidence for the former is present in Fig. 3. We observe that $NH_3$ production achieves a maximum when $H_2$ breakthrough occurs. At $H_2$ breakthrough, the effluent composition has a large excess of $H_2$ compared to NO. This suggests that the surface has a corresponding high H/N ratio. Such a condition would provide the route for $NH_3$ formation by the overall reaction:

$$NO + 2.5H_2 \leftrightarrow NH_3 + H_2O \quad (7)$$

Note that the selective reduction of NO with $H_2$ (6) is the linear combination of NO decomposition (1) and hydrogen oxidation (5), although this says nothing about the mechanistic pathway, which we examine in more detail below.

Knowledge of the source of NO is important in understanding the transient reduction process. Certainly NO from the gas phase may adsorb on Pt and decompose. However, in the current study NO is not present during the $H_2$ pulse, so it must originate as accumulated NO on Pt from a previous pulse or as a decomposition product from the barium storage component. The former is less likely; otherwise the results from the reduction of the Pt catalyst would bear more resemblance to the Pt/Ba catalyst, after NO storage; more recent experiments with Pt/$Al_2O_3$ shows negligible N storage over Pt at 350 °C. Furthermore, Nova et al. [24] have shown that the direct reaction between $H_2$ and barium nitrate is slow in the absence of Pt. On the other hand, while in the presence of Pt, the reduction is much faster. In keeping with the role of $H_2$ as a scavenger of adsorbed O, consider that the reverse of the storage steps leading to barium nitrate occur during reduction (i.e., (S11)–(S10)–(S9) or (S15)–(S14)–(S13)–(S12)). The first group of steps (S11)–(S10)–(S9) when combined give the overall reaction

$$Ba(NO_3)_2 + 4Pt \leftrightarrow BaO_2 + 2O{-}Pt + 2NO(-Pt) \quad (8)$$

This "catalytic" decomposition of $Ba(NO_3)_2$ produces adsorbed O, which reacts further with adsorbed H to form $H_2O$. Moreover, the NO product may decompose on the clean Pt or react with adsorbed H, forming $N_2$ or $NH_3$. The second group (S15)–(S14)–(S13)–(S12) when combined gives the overall reaction:

$$Ba(NO_3)_2 + NO(-Pt) + 2(Pt) \leftrightarrow BaO + 3NO_2(-Pt) \quad (9)$$

The $NO_2$ formed may decompose to NO and $O_2$, both of which can react with hydrogen. The overall reaction (9) requires the presence of NO during reduction to form $N_2$. Since reduction is carried out with pure $H_2$, reduction is more likely to occur via route (8) than (9).

With this overall mechanistic picture as a backdrop, the more specific features of the Pt/BaO/$Al_2O_3$ catalyst in the pump-probe experiments are now examined. The key factors determining the reaction pathways are the initial state of the catalyst (pre-reduced, pre-oxidized, pre-nitrated), the relative intensities of the NO and $H_2$ pulses (NO:$H_2$ feed ratio), and the composition and relative amounts of products formed during each pulse. Regarding the relative intensities of NO to $H_2$, we consider NO/$H_2$ = 1 to be the balance point corresponding to the stoichiometry of NO reduction by $H_2$ (6).

On a pre-reduced surface, with excess $H_2$ (NO:$H_2$ = 1:3.8, Fig. 4a), the first pulse of NO produces a stoichiometric amount of $N_2$ (NO pulse intensity is about $1.7 \times 10^{16}$ molecules/pulse for the duration of the experiment). The subsequent pulse of $H_2$ ($6.5 \times 10^{16}$ molecules/pulse), which is in stoichiometric excess, reacts with surface oxygen to form water, cleaning the surface. The excess $H_2$ conditions are effective in maintaining a clean Pt surface whereby little NO is stored on the barium storage component. No other species are observed to form on the surface, except a minor amount of ammonia. The fact that NO is not observed during the NO pulse (not shown) indicates that all the NO is consumed and forms $N_2$. The amount of $H_2$ consumed is about 1.16 times higher than NO consumed, which is close to the 1:1 ratio and within experimental error. This indicates the reduction of NO over Pt surface occurs via reaction (6). Since NO is first exposed to a reduced Pt surface, it decomposes to form $N_2$ (seen by its immediate and stoichiometric amount), leaving adsorbed O adatoms. The reaction sequence is essentially decomposition of NO over Pt surface followed by O–Pt reaction with two H adatoms to water (Eq. (1) and (5)). This is consistent with the study of Burch et al. [20] who have shown that NO reduction by $H_2$ does not occur by direct reaction between NO and $H_2$ but essentially occurs sequentially with NO decomposition followed by reduction of adsorbed oxygen by $H_2$.

When NO is in excess (NO:$H_2$ = 1:0.5, Fig. 4b; NO:$H_2$ = 1:0.34, Fig. 4c) there is a rapid falloff in the $N_2$ production during the NO pulse. These data suggest that there is insufficient $H_2$ to react away all of the surface oxygen, leaving residual oxygen for the next NO pulse. On the other hand, the emergence of $N_2$ production during the $H_2$ pulse signals the onset of the participation of NO that accumulates on the Pt or stores on the barium phase, as discussed above in connection with the NO pulse experiments (Fig. 1b). In the absence of gas phase $O_2$, NO storage may be initiated by the accumulating surface oxygen that reacts with BaO to form barium peroxide (S8) at the Pt–Ba interface. This is followed by the addition of gas phase or surface NO ((S9)–(S10)). Alternatively, $NO_2$ produced by reaction of adsorbed NO and the accumulating surface oxygen may migrate via the surface or through the gas phase to barium storage sites. During a subsequent $H_2$ pulse, Pt sites are freed up via hydrogen oxidation, initiating the catalytic decomposition of the nitrate (S11)–(S10)–(S9) or (S14)–(S13)–(S12), which supplies NO on Pt where decomposition and/or reduction occur. This interfacial mechanism between Pt–Ba is supported by the observed rapid increase in $N_2$ during the $H_2$ pulses. Eventually the $N_2$ produced during the $H_2$ pulse reaches a steady level which depends on the amount of $H_2$ fed. A separate more recent study on Pt/$Al_2O_3$ (to be published elsewhere) does not show significant storage of NO on Pt at 350 °C. Also, from the reduction of Pt/$Al_2O_3$ (Fig. 2), the amount of $N_2$ produced is significantly lower than that on Pt/Ba/$Al_2O$. Hence, the large production of $N_2$ during $H_2$ pulse in excess NO pump-probe experiment is an indication of NO coming from the storage component, viz., BaO. One important

observation is that NO storage occurs almost instantaneously after the first $NO/H_2$ cycle with $N_2$ production rapidly decreasing during the NO pulse. Since Pt sites are in large excess to the number of NO molecules fed during a pulse, the $N_2$ production should be sustained at a steady level until all of the Pt sites are occupied by oxygen. This clearly indicates that the process of NO storage is occurring on the Pt/Ba catalyst as soon as Pt–O is formed. Indeed, separate pump-probe experiments with $Pt/Al_2O_3$ in excess NO (not shown here) show a constant $N_2$ formation before it drops down.

When NO molecules are in excess some interesting trends are observed. For example, during the $NO:H_2 = 1:0.50$ experiment the $N_2$ production (during NO pulse) is equal to that of the $N_2$ production (during $H_2$ pulse) at essentially the point of NO breakthrough (specifically pulse number 407 in Fig. 4b). In this experiment $H_2$ is fed at approximately twice the level that $N_2$ is produced during the NO and $H_2$ pulses ($1.27 \times 10^{16}$ molecules $H_2$/pulse versus $6.1 \times 10^{15}$ $N_2$/pulse). NO breakthrough occurs when there are insufficient Pt sites to adsorb the input NO. In other words, when the NO fed exceeds a critical Pt site concentration, excess NO appears in the product. If we compare the total $N_2$ produced during the $H_2$ pulse to the amount of NO stored during the NO pulse, it is about 0.45, which is very close to stoichiometric amount of 0.5 (reaction (6)). The overall $N_2$ produced during both the NO and $H_2$ pulses approaches approximately 0.47 of the total NO fed during NO pulse. In essence, the $N_2$ production is by NO decomposition on Pt with the generated O–Pt consumed by $H_2$. The small difference of ~0.05 represents the stored NO on the surface. When less $H_2$ is fed (Fig. 4c) the same ratio of $N_2$ produced to NO fed is obtained. In this case, the cross-over of $N_2$ occurs in the region of NO breakthrough. Again, the amount of $N_2$ ($5.2 \times 10^{15}$ molecules/pulse) is roughly half the $H_2$ feed pulse intensity ($9 \times 10^{15}$ molecules/pulse). After the cross-over point, the production of $N_2$ during $H_2$ pulse reaches a steady value which indicates that there is insufficient $H_2$ fed to clean the Pt and to generate vacant sites. Another point to note is that $N_2$ production during the NO pulse continues to decrease, indicating that sites for NO adsorption and decomposition during the NO pulse are different than the sites for $N_2$ formation during $H_2$ pulse, lending credence to the picture of an interfacial reaction. The overall NO stored per pulse is higher in this case as compared to $NO:H_2$ ratio of 1:0.5, which is expected because of the reduced $H_2$ supply.

Ammonia formation was observed during all of the pump-probe experiments. The generation of ammonia during the pump-probe experiments conveys the interplay of several competing reactions. In an excess of $H_2$ ($NO/H_2 = 1/1.8$), ammonia formation is not observed until the 60th pulse while no such lag is observed at reduced $H_2$ feed rates ($NO/H_2 = 1/0.5$, Fig. 4b; 1/0.34, Fig. 4c). This suggests that the large excess of $H_2$ is effective in maintaining a clean Pt surface for NO decomposition during the NO pulse. The eventual appearance of $NH_3$ suggests that a gradual accumulation of NO on the barium phase which provides NO later in the experiment via the barium nitrate decomposition. This is in contrast to the lower $H_2$ feed rate experiments which show an immediate generation of $NH_3$. In those experiments, the accumulation of surface oxygen leads to a larger fraction of NO storing on the barium phase. As a result, subsequent pulses of $H_2$ produce ammonia. After a large number of pulses (>500) a pseudo steady state is achieved in which the ammonia formation rate is an increasing function of the feed $H_2$ concentration (or decreasing function of $NO/H_2$). This trend is not surprising since the stoichiometric requirement for ammonia production is $NO/H_2 = 1/2.5$ (reaction (7)). The catalyst approaches a constant state when the supply of N from NO is balanced by the supply of H from $H_2$. Another point that is worth noting is that $NH_3$ forms even under $H_2$ starved conditions, albeit to a lesser extent. Studies are currently being pursued to better understand the $NH_3$ formation mechanism.

On a pre-oxidized catalyst the effect of oxygen adatom inhibition is apparent during an initial number of pump-probe pairs of $NO/H_2$ ($NO = 2.40 \times 10^{16}$ molecules/pulse, $H_2 = 5.84 \times 10^{16}$ molecules/pulse). Initially little $N_2$ is formed during the NO pulse (Fig. 6b). It is also noted that there is no breakthrough of NO. These data confirm that NO does not decompose on the oxidized Pt surface but that it will accumulate, most likely by storage on the barium phase. With the excess $H_2$ feed most of the initial $N_2$ is produced exclusively during the $H_2$ pulse, and must originate from NO supplied from the storage component. $H_2$ is not evolved during its first few pulses since it is consumed in its reaction with the surface oxygen, both from the pre oxidation and oxygen produced from NO decomposition. By the 20th pulse the formation of $N_2$ is observed exclusively during the NO pulse, with corresponding $N_2$ during $H_2$ pulse reducing to a negligible level, indicating no more storage is possible since enough Pt sites are available for NO to decompose. The excess $H_2$ is then seen in the effluent (ca. 40th pulse). It is observed that $N_2$ production during the NO pulse quickly reaches a steady level which indicates the effectiveness of $H_2$ in cleaning Pt of oxygen, creating empty sites for NO decomposition/reduction.

The pre-nitrated catalyst exhibits behavior similar to the pre-oxidized Pt (storage = $1.61 \times 10^{-4}$ mol NO/g of catalyst). Under conditions of excess $H_2$ ($NO = 2.2 \times 10^{16}$ molecules/pulse, $H_2 = 6.92 \times 10^{16}$ molecules/pulse, $NO:H_2 = 3.14$) most of the $N_2$ is produced during the $H_2$ pulse during the initial stage (Fig. 7a). This indicates that the Pt is covered with oxygen, inhibiting NO decomposition during the NO pulse. However, the NO does not break through or decompose, indicating that it stores, assisted by the surface oxygen through one of the two mechanisms described earlier. On the other hand, during the $H_2$ pulse $N_2$ production is observed, which is likely a result of catalytic decomposition of the nitrite/nitrate at vacant Pt sites created by hydrogen oxidation, followed by NO spillover and decomposition. With the excess $H_2$ there is a rapid recovery of the catalyst such that $N_2$ generated during the NO pulse reaches a constant level by the ca. 30th pulse. It is interesting that $N_2$ continues to be formed during the $H_2$ pulse for about 100 pump-probe cycles, which is reduction of NO that has stored on the catalyst. The amount of nitrate pre-stored on the catalyst and the hydrogen pulse intensity determine the duration of this transient.

A more detailed analysis of the data (Fig. 7b) suggests that NO decomposition occurs on reduced Pt sites whereas the reduction

of stored NO essentially occurs at the Pt–Ba interface. During the first NO pulse a small but measurable amount of NO is observed, while there is almost no production of $N_2$, indicating that storage is occurring. The storage may be facilitated by the oxygen occupying the Pt sites from the pre-nitration. The subsequent $H_2$ pulse produces $N_2$ but there is no detectable $H_2$, indicating that all of the $H_2$ is consumed. As the Pt sites are cleaned of adsorbed oxygen, pulsed NO eventually finds sites to decompose and form $N_2$ as revealed by the increasing $N_2$ intensity. At about the 30th pulse $N_2$ produced during the NO pulse is about half the amount of NO fed. This indicates that when a critical fraction of Pt sites is reduced by $H_2$, NO will adsorb and decompose. This pathway competes with the storage pathway. Even under conditions in which most of the NO decomposes during the NO pulse, $N_2$ continues to be produced during the $H_2$ pulse, the N source of which is the Ba storage phase. The decomposition of stored NOx (overall reaction (8)) produces NO, which spills over from the Ba phase to the Pt and decomposes, producing O adatoms. The Pt–O react with H during the subsequent $H_2$ pulse which is completely consumed as evidenced by the lack of $H_2$ in the effluent. When the amount of stored NO drops below a critical level, no more surface oxygen is provided, and $H_2$ breakthrough occurs during the $H_2$ pulse. At that point the process follows the typical pump-probe on a reduced catalyst surface (Fig. 4a). This explains the late breakthrough of $H_2$ even though $N_2$ production occurring during the NO pulse attains the stoichiometric value indicative of decomposition (the difference between NO in and $N_2$ out is considered within experimental error in light of data from other pump-probe experiments in excess of $H_2$). It is noted that the total $N_2$ generated beyond the 30th pulse is $2.65 \times 10^{-5}$ mol N/g cat, which is close to the value obtained for the reduction experiment in Fig. 2. This supports the speculation that $N_2$ produced during the $H_2$ pulse essentially comes from the storage component and occurs at the Pt–Ba interface.

In pump-probe experiments on the pre-nitrated catalyst involving an excess of NO (NO = $2.60 \times 10^{16}$ molecules/pulse, $H_2 = 9.0 \times 10^{15}$ molecules/pulse) there is a break-in period with an approach to a pseudo steady state. Initially there is no $N_2$ produced during the NO pulse indicating that NO stores to some extent, forms $N_2O$ as a secondary product with the remainder appearing in the effluent. The next $H_2$ pulse cleans the surface to produce $N_2$ from the stored N. The amount of $H_2$ observed during the $H_2$ pulse is at the detection limit. As NO stores, the production of $N_2O$ increases. This suggests that reduction with $H_2$ makes available Pt sites for NO to decompose to form $N_2$ and $N_2O$, which increase to steady levels. Most of the nitrogen is produced during the $H_2$ pulse over the entire 2250 pulse experiment. Comparatively little $N_2$ is produced during the NO pulse which indicates that insufficient $H_2$ is fed to react away the surface oxygen. $N_2O$ formation is more pronounced under these conditions, indicating the selectivity is higher in an excess of NO. The production of $NH_3$ is also higher in these experiments compared to other pump-probe experiments (data not shown here) indicating that most of the N stored on the surface participates via this route. In essence, additional NO stores and forms $NH_3$ during the $H_2$ pulse, an observation consistent with previous pump-probe experiments and experiments involving storage where the catalyst is nearing saturation (Fig. 1b).

## 5. Conclusions

We have conducted a systematic TAP study of the transient NO storage and reduction on model Pt and Pt/Ba supported catalysts under near isothermal conditions. Our study shows a complex interplay between the storage and reduction processes involving several overall reactions. Our findings are consistent with the picture of a precious metal/storage component interface-driven process during NO storage and reduction.

NO pulsing experiments in the absence of gas phase $O_2$ reveal that NO will either decompose on Pt or store through the active participation of accumulating oxygen adatoms which spill over and oxidize BaO, or react with NO to form $NO_2$, which subsequently stores on BaO. Either route leads to stored nitrite/nitrate which provides a source of NO during subsequent reduction. On a clean Pt surface NO decomposition occurs readily, forming mostly $N_2$ and adsorbed O species. NO decomposition can be sustained if sufficient reductant $H_2$ is supplied to maintain a clean Pt surface.

$NO/H_2$ pump-probe experiments show how the catalyst responds to different initial states and $NO/H_2$ feed ratios. During exposure to $H_2$ under the isothermal low pressure conditions of the TAP, the NOx stored at the Pt/Ba interface is reduced by reverse spillover of NO from the Ba compound to Pt crystallites, while reduction of NOx stored further from the interface is apparently more difficult [24]. The reduction takes place at the Pt–Ba interface and since the conditions are isothermal, there is no thermal decomposition of Ba nitrite/nitrate to supply NO from gas phase. This is supported by the production of $N_2$ during the $H_2$ pulse in NO–$H_2$ pump-probe experiments on clean Pt (Fig. 4b and c) and on pre-nitrated Pt (Fig. 7a and b).

The role of the barium storage component is to supply NO to the Pt during the reduction step. Pump-probe experiments show minimal storage of NO in excess $H_2$ because of the effectiveness of the clean Pt in catalyzing the NO decomposition. The $N_2$ produced during NO decomposition (NO pulse) is maintained at a steady level indicating that the Pt surface is regenerated continuously during the intermittent $H_2$ pulse. In an excess of NO a steady decrease in the $N_2$ production occurs during the NO pulse because of the inhibition by the adsorbed O species and its participation in the storage of NO. As O accumulates the storage of NO becomes more significant, made evident by the increased $N_2$ production during the $H_2$ pulse. The immediate decrease in $N_2$ during the NO pulse and generation of $N_2$ during the $H_2$ pulse indicates that storage is a fast process and occurs as soon as O accumulates on the Pt. The $N_2$ production reaches a steady level depending upon the amount of $H_2$ introduced during the $H_2$ pulse.

The pump-probe data also suggest that NO conversion to $N_2$ occurs at two different sites. The first site is the bulk Pt surface that is readily cleaned by $H_2$ which leads to immediate formation of $N_2$ from NO during the NO pulse. The second site is in the close proximity of the Pt/Ba interface and is involved in the sequential hydrogen oxidation, nitrate decomposition, and

NO decomposition/reduction. On a pre-nitrated surface, we observe that $N_2$ production during the NO pulse reaches a steady value quickly. $N_2$ is also produced at a constant rate during the subsequent $H_2$ pulse. Once these sites are depleted of adsorbed NO, NO stored as nitrite/nitrate spills over to form $N_2$ by NO decomposition. $H_2$ breakthrough occurs only when the stored NOx on Ba cannot be further reduced. This picture is consistent with the recent spectroscopic study by Sakamoto et al. [13] who showed for model Pt/BaO catalysts that the storage and reduction of NOx occurs at the Pt/BaO interface.

The exhaust of lean-burn and diesel vehicles produces a large surplus of gas phase $O_2$. In this study oxygen was supplied by the NO or by pre-treatment by $O_2$ or NO. The role of gas phase $O_2$ is the subject of ongoing TAP studies and will be reported elsewhere.

Finally, complementary modeling is needed to discriminate between alternate mechanistic pathways and to estimate kinetic parameters. This work is ongoing and will be presented elsewhere.

## Acknowledgements

The financial support of Engelhard Inc. and the State of Texas Coordinating Board Technology Development and Transfer grant program is gratefully acknowledged. This material is also based upon work supported by the Department of Energy under Award No. DE-FC26-05NT42630. We also acknowledge helpful discussions with Stan Roth and Yuejin Li at Engelhard.



## References

[1] S.I. Matsumoto, Catal. Today 29 (1996) 43.
[2] S.I. Matsumoto, Cattech 4 (2000) 102.
[3] N. Takahashi, H. Shinjoh, T. Iijima, T. Suzuki, K. Yamazaki, K. Yokota, H. Suzuki, N. Miyoshi, S.I. Matsumoto, T. Tanizawa, T. Tanaka, S.-S. Tateishi, K. Kasahara, Catal. Today 27 (1996) 63.
[4] D. James, E. Fourre, M. Ishii, M. Bowker, Appl. Catal. B Environ. 45 (2003) 147.
[5] K. Kabin, P. Khanna, R.L. Muncrief, V. Medhekar, M.P. Harold, Catal. Today 114 (2006) 72.
[6] K.S. Kabin, R.L. Muncrief, M.P. Harold, Y. Li, Chem. Eng. Sci. 59 (2004) 5319.
[7] R.L. Muncrief, P. Khanna, K.S. Kabin, M.P. Harold, Catal. Today 98 (2004) 393.
[8] L. Olsson, E. Fridell, J. Catal. 210 (2002) 340.
[9] L. Olsson, H. Persson, E. Fridell, M. Skoglundh, B. Andersson, J. Phys. Chem. B 105 (2001) 6895.
[10] L. Castoldi, I. Nova, L. Lietti, P. Forzatti, Catal. Today 96 (2004) 43.
[11] H. Mahzoul, J.F. Brilhac, P. Gilot, Appl. Catal. B Environ. 20 (1999) 47.
[12] A.J. Paterson, D.J. Rosenberg, J.A. Anderson, Stud. Surf. Sci. Catal. 138 (2001) 429.
[13] Y. Sakamoto, K. Okumura, Y. Kizaki, S. Matsunaga, N. Takahashi, H. Shinjoh, J. Catal. 238 (2006) 361.
[14] I. Nova, L. Castoldi, L. Lietti, E. Tronconi, P. Forzatti, F. Prinetto, G. Ghiotti, Soc. Automot. Eng. SP-1942 (2005) 221.
[15] M. Sharma, K. Kabin, M. P. Harold, V. Balakotaiah, Soc. Automot. Eng. SP-1940 (2005) 275.
[16] R. Burch, P. Fornasiero, B.W.L. Southward, J. Catal. 182 (1999) 234.
[17] D.K. Captain, C. Mihut, J.A. Dumesic, M.D. Amiridis, Catal. Lett. 83 (2002) 109.
[18] W.S. Epling, J.E. Parks, G.C. Campbell, A. Yezerets, N.W. Currier, L.E. Campbell, Catal. Today 96 (2004) 21.
[19] S. Lacombe, J.H.B.J. Hoebink, G.B. Marin, Appl. Catal. B Environ. 12 (1997) 207.
[20] R. Burch, P.J. Millington, A.P. Walker, Appl. Catal. B Environ. 4 (1994) 65.
[21] I. Nova, L. Castoldi, L. Lietti, E. Tronconi, P. Forzatti, F. Prinetto, G. Ghiotti, J. Catal. 222 (2004) 377.
[22] L. Castoldi, I. Nova, L. Lietti, P. Forzatti, Prog. Catal. Res. (2005) 199.
[23] T.J. Toops, D.B. Smith, W.S. Epling, J.E. Parks, W.P. Partridge, Appl. Catal. B Environ. 58 (2005) 255.
[24] I. Nova, L. Lietti, L. Castoldi, E. Tronconi, P. Forzatti, J. Catal. 239 (2006) 244.